

Journal Pre-proof

The correctness of van 't Hoff plots in chiral and achiral chromatography

Annamária Sepsey, Éva Horváth, Martina Catani, Attila Felinger

PII: S0021-9673(19)31002-7
DOI: <https://doi.org/10.1016/j.chroma.2019.460594>
Reference: CHROMA 460594



To appear in: *Journal of Chromatography A*

Received date: 1 July 2019
Revised date: 26 September 2019
Accepted date: 30 September 2019

Please cite this article as: Annamária Sepsey, Éva Horváth, Martina Catani, Attila Felinger, The correctness of van 't Hoff plots in chiral and achiral chromatography, *Journal of Chromatography A* (2019), doi: <https://doi.org/10.1016/j.chroma.2019.460594>

This is a PDF file of an article that has undergone enhancements after acceptance, such as the addition of a cover page and metadata, and formatting for readability, but it is not yet the definitive version of record. This version will undergo additional copyediting, typesetting and review before it is published in its final form, but we are providing this version to give early visibility of the article. Please note that, during the production process, errors may be discovered which could affect the content, and all legal disclaimers that apply to the journal pertain.

Highlights

- The van't Hoff plot analysis was tested for several chromatographic circumstances.
- Two columns were serially connected to get a system containing two adsorption sites.
- Theoretical considerations were made to show the non-additivity of ΔH and ΔS values.
- ΔH and ΔS values were plotted against the average pressure drop and extrapolated.

Journal Pre-proof

The correctness of van 't Hoff plots in chiral and achiral chromatography

Annamária Sepsey^{a,*}, Éva Horváth^a, Martina Catani^b, Attila Felinger^{a,c,d}

^aDepartment of Analytical and Environmental Chemistry and Szentágotthai Research Center, University of Pécs, Ifjúság útja 6, H-7624 Pécs, Hungary

^bDepartment of Chemical and Pharmaceutical Sciences, University of Ferrara, Ferrara, Italy

^cMTA-PTE Molecular Interactions in Separation Science Research Group, Ifjúság útja 6, H-7624 Pécs, Hungary

^dInstitute of Bioanalysis, Medical School, University of Pécs, Szigeti út 12, H-7624 Pécs, Hungary

Abstract

van 't Hoff plots (logarithm of the retention factor, $\ln k_{vs}$, vs. the reciprocal of absolute temperature, $1/T$) are commonly used in chromatographic studies to characterize the retention mechanisms based on the determined enthalpy (ΔH) and entropy (ΔS) change of analyte adsorption. In reversed phase liquid chromatography these thermodynamic parameters could help to understand the retention mechanism. In chiral chromatography, however, the conclusions drawn based on van 't Hoff plots can be deceptive because several different types of adsorption sites are present on the surface of stationary phase. The influence of heterogeneity, however, cannot be studied experimentally.

In this study, we employed two reversed phase columns with different retention mechanisms to show that by ~~serial connection of these~~ serially coupling the columns, the obtained thermodynamic parameters are not related to the results obtained on the ~~individual columns, respectively~~ respective individual columns. Furthermore, our results show that the experimental conditions – such as flow-rate or choice of instrument – will strongly influence the calculated enthalpy and entropy values.

Keywords: van 't Hoff plot, entropy change, enthalpy change, adsorption sites, chiral separation mechanism, thermodynamics

*Corresponding author, e-mail address: sepsey@gamma.ttk.pte.hu

23 1. Introduction

24 Chiral separations have become a rather important chromatographic area in
 25 both analytical and preparative separations. ~~Retention~~ The retention behavior
 26 in chiral separations is often investigated via the estimation of enthalpy and
 27 entropy changes of enantiomer separation to unfold the mechanism of chiral
 28 recognition. In a typical case, several chemically related chiral analytes are
 29 involved and their retention is studied using a series of systematically changed
 30 experimental conditions. Nevertheless, it is nowadays clear that despite the
 31 simplicity of the van 't Hoff analysis, even the physical interpretation of its
 32 parameters is limited because the chromatographic column is an open system
 33 with constant pressure gradient, i.e. neither isobaric nor isochoric [1].

34 ~~On the surface of chiral stationary phases, different types of adsorption sites~~
 35 ~~(i.e. various enantioselective and nonselective sites) are present [2, 3], and the~~
 36 ~~van 't Hoff procedure uses only the retention factor derived from the retention~~
 37 ~~time of a retained and that of a non-retained compound to describe the bonding~~
 38 ~~of an analyte to the stationary phase. Thus the individual bondings and their~~
 39 ~~actual ratio in the chromatographic column are never determined and the conclusions~~
 40 ~~drawn on the basis of the thermodynamic data derived can easily be deceptive.~~

41

The van 't Hoff analysis used in chromatographic practice is based on the equation

$$\ln k = -\frac{\Delta H}{RT} - \frac{\Delta H^\circ}{RT} + \frac{\Delta S}{R} - \frac{\Delta S^\circ}{R} + \ln \phi, \quad (1)$$

42 where k is the retention factor of the ~~observed peak~~, ~~ΔH and ΔS are the analyte,~~
 43 ~~ΔH° and ΔS° are the standard molar~~ enthalpy and entropy changes, ~~respec-~~
 44 ~~tively,~~ R is the gas constant, T is the temperature and ϕ is the phase ratio (i.e.
 45 the ratio of the volume of the stationary phase and that of the mobile phase).
 46 This method assumes that by plotting $\ln k$ against $1/T$ a linear relationship is
 47 obtained. ~~ΔH ΔH° is calculated from the slope~~ while ~~ΔS ,~~ ~~whereas ΔS° is de-~~
 48 ~~rived from the intercept of Eq. 1.~~

49 ~~On the surface of chiral stationary phases, different types of adsorption sites~~
 50 ~~(i.e. various enantioselective and nonselective sites) are present [2, 3], and the~~
 51 ~~van 't Hoff procedure uses only the retention factor derived from the retention~~
 52 ~~time of a retained and that of a non-retained compound to describe the interaction~~
 53 ~~of an analyte with the stationary phase. Thus the individual interactions and~~
 54 ~~their actual ratio in the chromatographic column are never determined and the~~
 55 ~~conclusions drawn on the basis of the derived thermodynamic data can easily~~
 56 ~~be deceptive.~~

57 Using a van 't Hoff plot in chiral chromatography such as the one illustrated
 58 in Fig. 2, several simplifications are made: the retention factor (k) does not refer
 59 to a single ~~bonding type of interaction~~ even in reversed phase chromatography
 60 [4, 5], and definitely not in chiral chromatography [3, 6–8] and the ~~true~~ phase
 61 ratio (ϕ) is actually never known [8–10].

62 Although Lämmerhofer [8] pointed out that the ~~the~~ information content
 63 of the thermodynamic studies and derived quantities is strongly limited and
 64 Asnin et al. [1] collected and demonstrated all the pitfalls possibly occurring
 65 when using van 't Hoff plots in chiral chromatography, there ~~are is~~ a great
 66 number of studies which favorably use it. It should be ~~mentioned,~~ ~~noted~~

67 that when using the logarithm of the ~~selectivity, the errors made during the~~
 68 ~~calculations cancel each other and the phase ratio also disappears~~ separation
 69 factor (selectivity) and not the retention factor, the error introduced by the
 70 unknown phase ratio is eliminated. This argument, however, does not apply to
 71 ~~calculating the calculation of~~ molar enthalpies and entropies of the heterogeneous
 72 adsorption process where the errors are still present.

73 In this work ~~we want to, we~~ show the importance of distinguishing between
 74 the adsorption sites present in ~~the a~~ chromatographic column. To achieve this,
 75 we ~~used use~~ achiral conditions. The serial connection of two reversed phase
 76 columns ~~and caffeine as analyte. By serially connecting the columns, results in~~
 77 a stationary phase with two ~~adsorption sites was obtained~~ different adsorption
 78 sites where both sites ~~were are~~ characterized individually using the van 't Hoff
 79 analysis. We also want to draw attention on instrumental and experimen-
 80 tal circumstances that highly influence the results derived from van 't Hoff
 81 ~~plots~~ analysis.

82 2. Theory

83 2.1. ~~Effect~~ The effect of two adsorption sites by column connection

For chiral stationary phases – where at least two types of adsorption sites are present – the retention factor is generally written [3] as the sum of the retention factor of the non-selective sites (ns) and that of the ~~selective sites such~~ enantioselective sites (es) as

$$k_{\text{exp}} = k_{\text{ns}} + k_{\text{es}}. \quad (2)$$

84 ~~By~~ Because the isolation of the selective and non-selective sites is not possible
 85 experimentally, we study a system containing two different reversed phase
 86 columns that are serially connected. This way, although, the results will not be
 87 based on chiral separations, we can get valuable information about a system
 88 where two different adsorption sites are present.

By the serial coupling of the columns, the expected retention time will be the sum of the individual retention times and also the void time is the sum of the respective void times. Thus, the retention factor of the ~~peak measured~~ analyte on the connected columns ~~must will~~ be

$$k = \frac{(t_{R,1} + t_{R,2}) - (t_{0,1} + t_{0,2})}{t_{0,1} + t_{0,2}}, \quad (3)$$

where $t_{R,1}$ and $t_{R,2}$ refer to the retention time of the same compound obtained on the first and the second column, while $t_{0,1}$ and $t_{0,2}$ are the void times of the first and second column, respectively. It follows that ~~by~~ using the individual retention factors to derive the retention times, $t_{R,i} = t_{0,i}(k_i + 1)$, Eq. 3 will simplify to

$$k = \frac{t_{0,1}k_1 + t_{0,2}k_2}{t_{0,1} + t_{0,2}}, \quad (4)$$

89 thus the overall retention factor is calculated as the void-time weighted average
 90 of the respective k values.

By substituting Eq. 4 to Eq. 1 and using the individual enthalpy and entropy changes calculated for the corresponding columns (i.e. ~~ΔH_T and ΔS_T~~ ΔH_i° and

ΔS_1° of the first column and ΔH_2 and ΔS_2 , ΔH_2° and ΔS_2° of the second column obtained using Eq. 1) one will get the following expression

$$k = \frac{V_{S,1} \exp\left(-\frac{\Delta H_1}{RT} + \frac{\Delta S_1}{R}\right) + V_{S,2} \exp\left(-\frac{\Delta H_2}{RT} + \frac{\Delta S_2}{R}\right)}{V_M} \frac{V_{S,1} \exp\left(-\frac{\Delta H_1^\circ}{RT} + \frac{\Delta S_1^\circ}{R}\right) + V_{S,2} \exp\left(-\frac{\Delta H_2^\circ}{RT} + \frac{\Delta S_2^\circ}{R}\right)}{V_M}, \quad (5)$$

91 where we already used that $\phi_1 V_{0,1} = V_{S,1}$ and $\phi_2 V_{0,2} = V_{S,2}$ and $V_M = V_{0,1} + V_{0,2}$
 92 is the mobile phase volume of the system. It is obvious from Eq. 5 that the en-
 93 thalpy and entropy values of two adsorption sites can not cannot be summed
 94 as it is assumed in chiral chromatography and or whenever the adsorption is
 95 heterogeneous.

96 3. Experimental

97 The mefloquin mefloquine profiles were acquired using a Shimadzu HPLC
 98 system including a binary pump and diode-array detector using ACN/MeOH/H₂O
 99 49/49/2 with 50 mM HCOOH and 30 mM HCOONH₄ as eluent in isocratic
 100 mode. Concentration of the sample was 0.1 mg/mL. 2 μ L was injected, the
 101 flow-rate was set to 1.0 mL/min. The column was a Chiralpak ZWIX(+) with
 102 a particle diameter of 3 μ m and dimensions of 4.6 \times 150 mm. Temperature
 103 was set to 20, 25, 30 and 35 $^\circ$ C to obtain the profiles. Detection was done at
 104 280 nm. The void time was obtained by injecting 1,3,5-tri-tert-butylbenzene
 105 (97+%, ThermoFisher GmbH). The mefloquine standard was purchased from
 106 Merck as hydrochloride salt with a purity of >98%. The molecular formula is
 107 C₁₇H₁₆F₆N₂O \cdot HCl.

108 The column connection experiments were carried out on a Waters Acquity
 109 I Class instrument (Waters Corporation, Milford MA, USA). The system con-
 110 sists of a binary solvent manager, an autosampler with a flow-through-needle
 111 injector, a column manager, a diode-array detector and a computer data station
 112 running Empower 3 software.

113 Two reversed phase columns were used to perform the experiments: a Zor-
 114 bax Eclipse Plus C18 (3.5 μ m; 4.6 \times 100 mm) and a Zorbax SB-CN (3.5 μ m;
 115 4.6 \times 150 mm) column. The mobile phase was MeOH/H₂O 25:75 (V/V%).
 116 The sample contained caffeine ($c_{inj} = 0.05$ mg/mL, >99%, Fluka Analytical)
 117 and thiourea ($c_{inj} = 0.06$ mg/mL, >99%, Sigma-Aldrich) dissolved in mobile
 118 phase and the injected volume was 0.5 μ L. The flow-rate was varied between
 119 0.1 and 0.7 mL/min, at each temperature (25, 30, 35, 40, and 45 $^\circ$ C). The sample
 120 contained caffeine ($c_{inj} = 0.05$ mg/mL) and thiourea ($c_{inj} = 0.06$ mg/mL) dissolved
 121 in mobile phase; $V_{inj} = 0.5$ μ L. Thus the separations were performed at 13 flow-
 122 rates and at 5 different temperatures to obtain the van 't Hoff plots for each
 123 column and when the columns were serially connected. Detection was done at
 124 272 nm.

125 To obtain the retention factors, the retention times were obtained using
 126 PeakFit v4.12 software by fitting exponentially modified Gaussian functions
 127 to the peaks. Then the retention times were corrected. The correction contains
 128 instrumental values such as system volume and injection drift by increasing
 129 the flow-rate. The values used for the correction are summarized in Table 1.

130 **4. Results and discussion**

131 4.1. *Mefloquin-Mefloquine* measurements

132 The retention behavior of mefloquine enantiomers on a ZWIX(+) column
 133 is rather unusual when carried out at several temperatures, as it is shown in
 134 Fig. 2. We can see that the retention of the first peak does not depend on the
 135 temperature and the second peak has significant tailing even using elevated
 136 temperatures. One would first assume overloading effects or slow adsorption–
 137 desorption kinetics [7], the situation is indeed rather complicated. From the
 138 peak shapes of the second peak shown on Fig. 2 we can conclude that several
 139 adsorption sites are present on this stationary phase.

140 The van 't Hoff analysis based on Eq. 1 shows that there is ~~one order of~~
 141 ~~magnitude difference in ΔH between the two peaks (2.41 a big difference in~~
 142 ~~ΔH° (-2.41 kJ/mol vs ~~23.8~~ -23.80 kJ/mol, ~~calculated via Eq. 1).~~ The) and in~~
 143 ~~ΔS° (-2.51 J/(K mol) vs. -62.40 J/(K mol)) values for the two enantiomers.~~
 144 The van 't Hoff plots are presented in Fig. 3, while the chemical structure
 145 of the mefloquine enantiomers and the ZWIX(+) selector are shown in Fig. 1.
 146 These energies however could not refer to a single bond, even one H-bond
 147 ~~could~~ would be larger, and based on the molecule structure, two or more H-
 148 bonds can ~~formed~~ form between one molecule and one stationary phase lig-
 149 and. There are several other possible interactions like such as ionic-bonding, π -
 150 stacking, enantiomer recognition, and it is also feasible that several molecules
 151 bond at the same time to one stationary phase ligand. ~~It is also interesting to~~
 152 ~~observe that the peak~~ As mentioned, it is interesting that the retention time of
 153 the less retained enantiomer does not change ~~by significantly when~~ increasing
 154 the temperature. This phenomenon is still unclear. Maybe one or more in-
 155 hibitory ~~bonds~~ interactions are also present and their ~~interaction~~ combination
 156 is balanced by temperature change.

157 The peak shape observed for the second eluted enantiomer can only occur
 158 when at least three different adsorption sites are present [11]. Using the stochastic
 159 theory of chromatography [12], the fitting of the characteristic function accounting
 160 for three adsorption sites is possible in the Fourier domain. This was carried
 161 out using an algorithm written in-house in Fortran programming language. It
 162 was assumed that the first eluted enantiomer is retained by only one type of
 163 adsorption site while the second eluted enantiomer is retained by all the three
 164 sites. The fitting procedure provides the number of adsorption-desorption
 165 steps and the average time that a molecule spends bound to the stationary
 166 phase for each adsorption site.

For a three-site retention process, the retention factor is written as

$$k = \frac{t'_R}{t_0} = \frac{n_1 \tau_1 + n_2 \tau_2 + n_3 \tau_3}{t_0} \quad (6)$$

167 where n_i is number of adsorption–desorption steps and τ_i the average sojourn
 168 time in the stationary phase during a single adsorption step on site i . The
 169 contribution of site i to the overall retention factor is $k_i = n_i \tau_i / t_0$.

170 From those results, the van 't Hoff plots of the individual adsorption sites
 171 can be obtained respectively. Table 2 contains the ΔH° and ΔS° values obtained
 172 from the chromatograms of the mefloquine enantiomers using the data obtained
 173 by the fitting procedure. While looking at the data presented in Table 2 it is

174 clear that there is a huge difference between the various sites, thus the overall
 175 ΔH° and ΔS° values obtained using retention factors cannot describe well the
 176 separation mechanism.

177 4.2. Theoretical van 't Hoff considerations

178 The retention data of the mefloquine ~~measurement~~ measurements were uti-
 179 lized to show the effect of more than one ~~bonding sites~~ type of interactions
 180 on the calculated thermodynamic parameters (ΔH and ΔS). ~~For the ΔH° and~~
 181 ~~ΔS° .~~ Although three adsorption sites and interactions were used in the fitting
 182 procedure, for the sake of simplicity only two sites were assumed. ~~The partitioning~~
 183 ~~of the retention factor was done based on the data obtained for the~~ are assumed
 184 in this theoretical part of the study.

185 We artificially partitioned the retention factor of the more retained meflo-
 186 quine enantiomer. ~~These k values were artificially partitioned~~ into certain per-
 187 centages to obtain k_1 and k_2 . To preserve the experimental behavior of the
 188 retention factor data e.g. k decreases as temperature is increased, we needed to
 189 partition the original data in different degrees at different temperatures. This
 190 is illustrated in Fig. 4 where k_1 is 60% of the original k value at 293 K thus k_2
 191 is 40% while at 308 K k_1 is 90% of the original k and k_2 is only 10% of it. At
 192 intermediate temperatures, the percentage of the partitioning yields that the
 193 logarithm of both k_1 and k_2 becomes linear as plotted against the reciprocal of
 194 temperature (shown in Fig. 5).

195 From the partitioned retention factors, a van 't Hoff plot was ~~made and~~
 196 ~~ΔH and ΔS created and ΔH° and ΔS°~~ were calculated. We should note at this
 197 point that for all entropy calculations the same phase ratio was ~~used~~ assumed
 198 to show the differences that are present only because of the partitioning.

199 To change the proportion of k_1 related to the original k , the $\ln k_1$ vs. $1/T$
 200 lines obtained from the partitioned data (indicated by squares in Fig. 4) were
 201 shifted while $\ln k_2$ was unchanged and both the ~~ΔH ΔH° - ΔS ΔS°~~ and the
 202 corresponding k_1 and k values were calculated. This shifting procedure was
 203 repeated for several cases. The ~~result are illustrated~~ calculated thermodynamic
 204 values are plotted against k_1/k shown in Figs. 6 and 7 ~~for the calculated enthalpy~~
 205 ~~and entropy changes, respectively.~~ The values obtained using Figs. 4 and 5 are
 206 at $k_1/k=0.6$ when the partitioning procedure was k_1 60% \rightarrow 90%.

207 The colors in Figs. 6 and 7 represent different partitioning procedures and
 208 it is indicated from which ~~rate constant~~ retention factor the thermodynamic
 209 data was calculated. It is obvious from these graphs that the ~~ΔH and ΔS ΔH°~~
 210 ~~and ΔS°~~ values calculated from the partitioned retention factors k_1 and k_2 only
 211 agree with the ones calculated from the original retention factor, k when the
 212 other type of adsorption site is not present, i.e. $k_1 = k$ or $k_2 = k$. When a
 213 heterogeneous interaction is assumed, the overall thermodynamic parameters
 214 calculated from the retention factor k show a nonlinear transition between k_1
 215 and k_2 .

216 4.3. Experiments with two adsorption sites

217 In chiral separations, one ~~can not~~ cannot eliminate the heterogeneity of the
 218 retention mechanism. Therefore when one wants to study how two or more
 219 interactions contribute to the overall retention, a simpler model system should
 220 be constructed. We designed a series of experiments using two reversed phase

221 columns of different retention mechanisms (but of the same inner diameter)
 222 to draw attention on the phenomenon discussed in the previous sections of
 223 this study. Separations were performed on each column separately and on the
 224 serially connected columns ~~as~~ as well. The conclusions drawn are general for
 225 other separation mechanisms, thus also for chiral chromatography ~~as well~~.

226 The first thing to decide when determining the thermodynamic parameters
 227 via the van 't Hoff procedure is whether or not the chromatographic circum-
 228 stances ~~—~~ such as flow-rate or back pressure ~~—~~ matter. To obtain a van 't
 229 Hoff plot, one has to measure the retention behavior of the compound under
 230 investigation, and that of a non-retained compound at various temperatures
 231 but ~~Figure Fig.~~ 8 illustrates that the retention factor depends on the flow-rate
 232 on Zorbax Eclipse C18 column. The same phenomenon was observed when
 233 using the Zorbax SB-CN column and also when we serially ~~connected~~ coupled
 234 the two columns.

235 The flow is generated via pressure across the chromatographic system, which
 236 results in higher pressure drops along the column as the flow-rate is increased.
 237 One should note that for two temperatures (25 and 30 °C), the for either individual
 238 and for the serially coupled columns the change of k shows a contradictory
 239 trend than expected ~~for both columns and also for the serially connected one~~
 240 (see Fig. 10). It has to be noted that this effect ~~can not~~ cannot be attributed to
 241 frictional heat. Frictional heat would result in a steep decrease in k as the flow-
 242 rate is increased. Our results at 25 °C, however, show a constant retention factor
 243 in the 0.5–0.7 mL/min flow-rate range. Furthermore, if we omit the results ob-
 244 tained at 25 °C, the van 't Hoff plots do not change significantly and the same
 245 thermodynamic values are calculated. When measuring and plotting classical
 246 van 't Hoff ~~plots~~ data, it is not common to use e.g. water bath to thermostat the
 247 column, so the problem of flow-rate presented here is a general warning.

248 In all three cases (with the two respective columns and ~~when serially connected~~
 249 ~~) for the serially connected one~~), the van 't Hoff plots were ~~drawn~~ created
 250 for each investigated flow-rate (Fig. 9). It is obvious from Fig. 9 that both the slope
 251 and the intercept depend on the particular flow-rates, thus the calculated en-
 252 thalpy and the entropy changes will differ as well. The pressure dependence
 253 of the retention is already known: even for small molecules, the pressure af-
 254 fects retention due to the change of the molar volume of the analyte during
 255 adsorption [13, 14].

256 As it was mentioned above, the calculation of the true phase ratio, ϕ is not
 257 possible in liquid chromatography. Even for the simplest case when only one
 258 bonding site is assumed on the surface of the stationary phase particles to be
 259 present, the ratio of the stationary phase and the mobile phase volumes ~~can not~~
 260 cannot represent the true phase ratio. Thus the ΔS - ΔS° values calculated not
 261 only in this study but in all van 't Hoff analyses in chromatography must be
 262 treated with reservations. The calculated thermodynamic values and the phase
 263 ratios are summarized in Table 3. The errors of the values (95% confidence
 264 limits) were calculated from regression data.

265 By connecting two columns serially, we get a heterogeneous stationary phase
 266 with two bonding sites, where the phase ratio should be known for the respec-
 267 tive sites. Thus, with a simple van 't Hoff plot, the true energy of a single
 268 ~~bonding can not~~ interaction cannot be determined. The data presented in Ta-
 269 ble 3 show that

- 270 • the calculated ΔH and ΔS ΔH° and ΔS° values vary with the flow-rate of
271 the separation;
- 272 • although similar values are obtained on the single columns, the thermo-
273 dynamic data calculated ~~when the columns were connected significantly~~
274 ~~for the serially coupled columns~~ differ from any of them;
- 275 • the values obtained for the connected columns are not between the re-
276 sults obtained for the single columns.

277 It is really interesting to investigate the correctness of Eqs. 4 and 5 and thus
278 the actual meaning of the thermodynamic parameters derived from the van 't
279 Hoff plots. Fig. 10 illustrates the correctness of Eq. 4. It is clear that these
280 equations describe the system well, for ~~every each~~ investigated flow-rate the
281 ~~percentage relative~~ difference between the calculated and measured values is
282 below 2.3% for Eq.4 and below 3.2% for Eq. 5.

The average ~~column~~ pressure is calculated ~~by as~~

$$p_{\text{avg}} = \frac{p_{\text{in}} + p_{\text{out}}}{2}, \quad (7)$$

283 where p_{out} was obtained as $p_{\text{system}} - p_{\text{detector}}$ so the pressure drop along the
284 detector cell was ~~subtracted subtracted~~ from the whole pressure drop. For
285 that ~~purpose~~, the detector was disconnected from the system and the pressure
286 was monitored for all flow-rates. To obtain p_{in} , both the column and the de-
287 tector were disconnected from the system and the pressure was ~~followed up~~
288 ~~along the flow-rates used~~ ~~determined for each flow-rate~~. Table 4 summarizes
289 the measured and calculated pressure data for ~~the~~ Zorbax SB-CN ~~column~~
290 at 25°C.

291 When one plots the ΔH and ΔS ΔH° and ΔS° values obtained at various
292 flow-rates against the average column pressure, a rather surprising result oc-
293 curs. The data shown in Tables 3 and 4 indicate that the thermodynamic pa-
294 rameters vary more or less linearly with the average pressure drop which is
295 shown in Figs. 11 and 12. Here not the linearity is emphasized but the change
296 with the flow-rate. The ΔH and ΔS ΔH° and ΔS° values for the serially con-
297 nected columns ~~can not cannot~~ be the combination of the individual results.

298 When the plots are extrapolated to $p = 0$ bar (dashed lines in Figs. 11
299 and 12) to eliminate the pressure effect, one gets ~~a more realistic~~ ΔH and ΔS
300 ~~more realistic~~ ΔH° and ΔS° values referring to the original van 't Hoff anal-
301 ysis. For ΔH ΔH° , the extrapolation to $p = 0$ results in ~~-16.8 -16.8~~ kJ/mol
302 whereas -8.5 kJ/mol is obtained at a widely used flow-rate 0.5 mL/min. For
303 ΔS ΔS° , the extrapolation to $p = 0$ results in ~~-43.2 -43.2~~ J/(K mol) whereas
304 ~~-15.8 -15.8~~ J/(K mol) is obtained at $F_v = 0.5$ mL/min. Thus it is ~~indeed~~
305 a problem that van 't Hoff ~~plot usually is~~ ~~plots are usually~~ determined at a sin-
306 gle flow-rate. Furthermore, results ~~are usually~~ obtained on different systems
307 or ~~at~~ different flow-rates are ~~usually~~ compared. Pressure has an important ef-
308 fect on the retention behavior and thus on the calculated thermodynamic pa-
309 rameters. ~~Heterogeneity Surface heterogeneity~~ further complicates the deter-
310 mination of the thermodynamic parameters. ΔH ΔH° values obtained on the
311 single columns are independent ~~and rather different~~ from the value obtained
312 on the serially connected columns. All the ~~ΔH and ΔS values~~ ΔH° and ΔS°
313 ~~values determined~~ in chromatography are only apparent, ~~it is not related to the~~

314 ~~bonding mechanisms~~ they do not express the true thermodynamic parameters
315 ~~of the interactions.~~

316 5. Conclusions

317 We have demonstrated that, however, in some cases interesting conclusions
318 can be drawn based on van 't Hoff plots [15, 16], the numerical molar thermo-
319 dynamic values determined from the slope and intercept of the van 't Hoff plot
320 can be erroneous because of the assumptions made compared to the original
321 van 't Hoff equation and because of the significant influence of the chromato-
322 graphic circumstances.

323 Both experimental and theoretical studies show that a more complex ther-
324 modynamic study of retention on any type of chromatographic stationary phase
325 is necessary than the one offered by van 't Hoff plots.

326 We have created a heterogeneous stationary phase containing two types of
327 adsorption sites by the serial connection of two columns. van 't Hoff analysis
328 has been used to calculate the thermodynamic parameters for the individual
329 sites and for the heterogeneous surface. It can be concluded that the hetero-
330 geneity of the stationary phase made the determination of the accurate ΔH
331 ~~and ΔS~~ ΔH° and ΔS° values impossible. That observation leads to a serious
332 constraint for van 't Hoff analysis in chiral chromatography, where stationary
333 phases are intrinsically heterogeneous.

334 Our results also show that pressure drop along the column will strongly
335 influence the calculated enthalpy and entropy values. Therefore, the value of
336 the calculated thermodynamic parameters strongly depend on the length of
337 the column, the particle size, ~~or the~~ flow-rate, or the instrument itself.

338 Acknowledgement

339 The work was supported by the NKFIH OTKA grant K125312 and by grant
340 GINOP-2.3.2-15-2016-00022. The work was also supported by the ÚNKP-18-3-
341 I-PTE-190 New National Excellence Program of the Ministry of Human Capac-
342 ities. ~~Special thanks to Martina Catani (University of Ferrara).~~

343 The project has been supported by the European Union, co-financed by the
344 European Social Fund Grant no.: EFOP-3.6.1.-16-2016-00004 entitled by Com-
345 prehensive Development for Implementing Smart Specialization Strategies at
346 the University of Pécs.

347 **References**

- 348 [1] L. D. Asnin, M. V. Stepanova, van't Hoff analysis in chiral chromatogra-
349 phy, *J. Sep. Sci.* 41 (2018) 1–19.
- 350 [2] T. Fornstedt, P. Sajonz, G. Guiochon, Thermodynamic study of an unusual
351 chiral separation. propranolol enantiomers on an immobilized cellulase, *J.*
352 *Am. Chem. Soc.* 119 (1997) 1254–1264.
- 353 [3] T. Fornstedt, P. Sajonz, G. Guiochon, A closer study of chiral retention
354 mechanisms, *Chirality* 10 (1998) 375.
- 355 [4] F. Gritti, G. Guiochon, A chromatographic estimate of the degree of het-
356 erogeneity of rplc packing materials 1. non-endcapped polymeric c30-
357 bonded stationary phase, *J. Chromatogr. A* 1103 (2006) 43–56.
- 358 [5] F. Gritti, G. Guiochon, A chromatographic estimate of the degree of sur-
359 face heterogeneity of reversed-phase liquid chromatography packing ma-
360 terials ii-endcapped monomeric c18-bonded stationary phase, *J. Chro-*
361 *matogr. A* 1103 (2006) 57–68.
- 362 [6] A. Cavazzini, L. Pasti, A. Massi, N. Marchetti, F. Dondi, Recent applica-
363 tions in chiral high performance liquid chromatography: A review, *Anal.*
364 *Chim. Acta* 706 (2011) 205–222.
- 365 [7] L. D. Asnin, Adsorption models in chiral chromatography, *J. Chromatogr.*
366 *A.* 1269 (2012) 3–25.
- 367 [8] M. Lämmerhofer, Chiral recognition by enantioselective liquid chro-
368 matography: Mechanisms and modern chiral stationary phases, *J. Chro-*
369 *matogr. A* 1217 (2010) 814–856.
- 370 [9] F. Gritti, G. Guiochon, Adsorption mechanisms and effect of temperature
371 in reversed-phase liquid chromatography. meaning of the classical van't
372 hoff plot in chromatography, *Anal. Chem.* 78 (2006) 4642–4653.
- 373 [10] T. L. Chester, J. W. Coym, Effect of phase ratio on van't hoff analysis in
374 reversed-phase liquid chromatography, and phase-ratio-independent es-
375 timation of transfer enthalpy, *J. Chromatogr. A* 1003 (2003) 101–111.
- 376 [11] A. Felinger, Mass transfer properties of zwitterionic chiral stationary
377 phases, Conference presentation at HPLC 2017 Prague (2017).
- 378 [12] A. Cavazzini, M. Remelli, F. Dondi, A. Felinger, Stochastic theory of
379 multiple-site linear adsorption chromatography, *Anal. Chem.* 71 (1999)
380 3453–3462.
- 381 [13] A. Felinger, B. Boros, R. Ohmacht, Effect of pressure on retention factors
382 in hplc using a non-porous stationary phase, *Chromatographia* 56 (2002)
383 S61–S64.
- 384 [14] I. Prauda, E. Bartó, A. Felinger, Influence of pressure on the retention of
385 resorcinarene-based cavitands, *J. Chromatogr. A* 1535 (2018) 123–128.

- 386 [15] I. Matarashvili, G. Kobidze, A. Chelidze, G. Dolidze, N. Beridze, G. Jibuti,
387 T. Farkas, B. Chankvetadze, The effect of temperature on the separation
388 of enantiomers with coated and covalently immobilized polysaccharide-
389 based chiral stationary phases, *J. Chromatogr. A* 1599 (2019) 172–179.
- 390 [16] M. Maisuradze, G. Sheklashvili, A. Chokheli, I. Matarashvili,
391 T. Gogatishvili, T. Farkas, B. Chankvetadze, Chromatographic and
392 thermodynamic comparison of amylose tris(3-chloro-5- methylphenylcar-
393 bamate) coated or covalently immobilized on silica in high-performance
394 liquid chromatographic separation of the enantiomers of select chiral
395 weak acids, *J. Chromatogr. A*, 1602 (2019) 228–236.

Journal Pre-proof

396 Tables

Table 1: Correction values at different flow-rates [on the Waters Acquity I Class instrument](#)

Flow-rate (mL/min)	Void Extracolumn time (s)	Void Extracolumn volume (μ L)
0.10	5.60	9.33
0.15	4.15	10.37
0.20	3.43	11.42
0.25	3.02	12.58
0.30	2.72	13.59
0.35	2.48	14.46
0.40	2.33	15.54
0.45	2.19	16.41
0.50	2.09	17.45
0.55	1.99	18.24
0.60	1.92	19.20
0.65	1.85	20.08
0.70	1.82	21.19

Table 2: [Thermodynamic values calculated from the data obtained during the fitting of the stochastic model for the three adsorption sites.](#)

	ΔH° kJ/mol	ΔS° J/(K mol)
1st site	-2.41	-2.51
2nd site	-31.10	-89.70
3rd site	-32.75	-123.30

Table 3: Calculated [phase ratios](#) and thermodynamic data for the Zorbax Eclipse C18, Zorbax SB-CN, and the serially connected columns at different flow-rates.

Flow-rate (mL/min)	C18		SB-CN		Connected		
	$\Delta H\phi$ (kJ/mol)	$\Delta H\Delta S^\circ$ J/(K mol)	$\Delta H\phi$ (kJ/mol)	$\Delta S\Delta S^\circ$ J/(K mol)	ϕ	ΔH° (kJ/mol)	ΔS° J/(K mol)
0.1	0.70	-14.27±0.40	-35.66±1.31	0.44	0.52	-15.01±1.04	-37.39±3.40
0.15	0.70	-13.83±0.68	-34.17±2.22	0.44	0.53	-14.18±0.82	-34.68±2.66
0.2	0.70	-13.08±1.08	-31.70±3.49	0.44	0.53	-13.34±0.95	-31.96±3.08
0.25	0.70	-12.42±1.56	-29.52±5.08	0.44	0.53	-12.39±1.19	-28.88±3.88
0.3	0.71	-11.85±1.85	-27.62±6.02	0.44	0.53	-11.57±1.45	-26.22±4.71
0.35	0.71	-11.19±1.56	-25.50±5.08	0.45	0.53	-10.78±1.60	-23.64±5.21
0.4	0.71	-10.52±1.02	-23.32±3.32	0.45	0.53	-10.03±1.85	-21.19±6.01
0.45	0.71	-10.07±0.98	-21.81±3.18	0.45	0.53	-9.31±2.51	-18.87±8.16
0.5	0.71	-9.64±0.85	-20.41±2.77	0.45	0.53	-8.55±2.62	-16.38±8.50
0.55	0.71	-9.32±0.56	-19.35±1.83	0.45	0.54	-8.31±1.59	-15.59±5.16
0.6	0.71	-9.01±0.33	-18.31±1.06	0.45	0.54	-7.98±1.80	-14.50±5.85
0.65	0.71	-8.60±0.22	-16.97±0.71	0.45	0.54	-7.76±2.75	-13.77±8.94
0.7	0.71	-8.18±0.47	-15.60±1.53	0.45	n/a	n/a	n/a

Table 4: Monitored and calculated pressures for Zorbax-SB-CN at 25°C at the investigated flow-rates. Pressures are shown in bar, while flow-rate is in mL/min. The shortened indices are: det.disc.=detector disconnected, col.disc.=column disconnected.

Flow-rate	p_{system}	$p_{\text{det.disc.}}$	$p_{\text{col.disc.}}$	p_{out}	p_{in}	p_{avg}
0.10	51	42	26	9	25	17
0.15	78	65	40	13	38	26
0.20	106	87	55	19	51	35
0.25	133	110	68	23	65	44
0.30	158	132	83	26	75	51
0.35	184	155	97	29	87	58
0.40	208	178	112	30	96	63
0.45	232	200	126	32	106	69
0.50	256	223	141	33	115	74
0.55	281	245	156	36	125	81
0.60	305	267	170	38	135	86
0.65	329	289	184	40	145	92
0.70	351	311	199	40	152	96

397 Figure captions

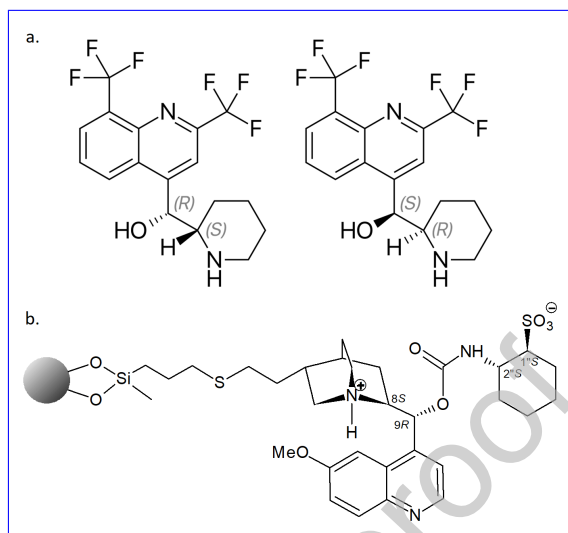


Figure 1: [a. Molecular formula of mefloquine enantiomers](#), [b. Molecular structure of ZWIX\(+\) selector](#).

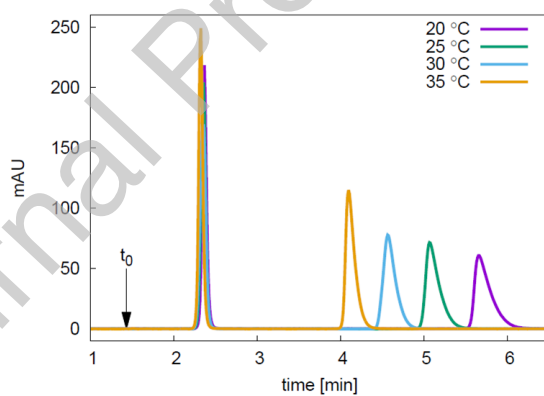


Figure 2: Chromatograms of mefloquine enantiomers recorded at different temperatures on a ZWIX(+) column.

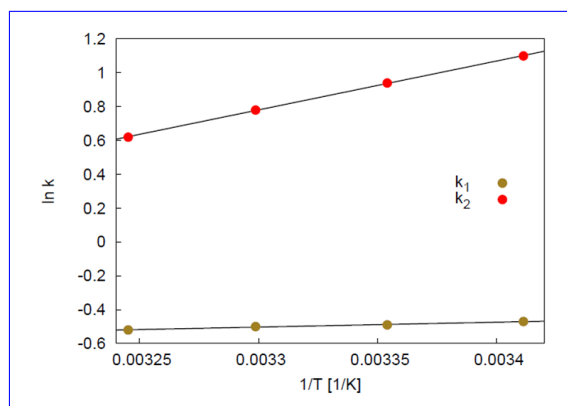


Figure 3: van't Hoff analysis plots of mefloquine enantiomers recorded at different temperatures on a ZWIX(+) column.

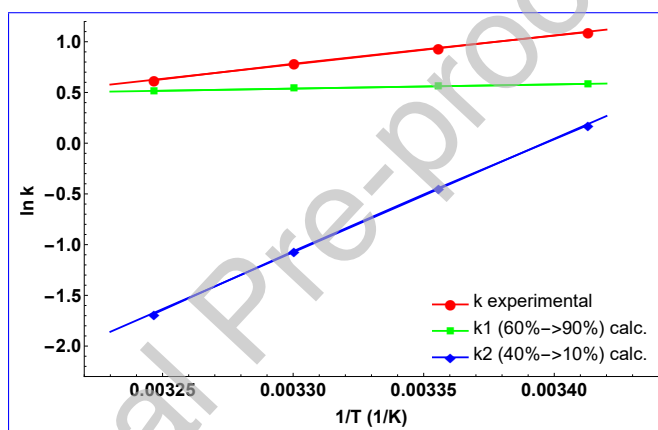


Figure 4: Example of theoretical partitioning the retention factor data. Red line shows the retention factors of the more retained mefloquin-mefloquine enantiomer used for the calculations while the blue and green lines are the arbitrary fractions of the experimental data.

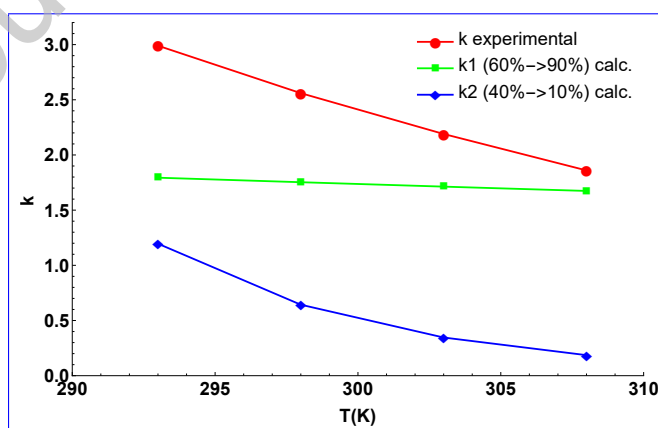


Figure 5: Plots of the partitioned and original retention factors shown in Fig. 4 used for the calculations.

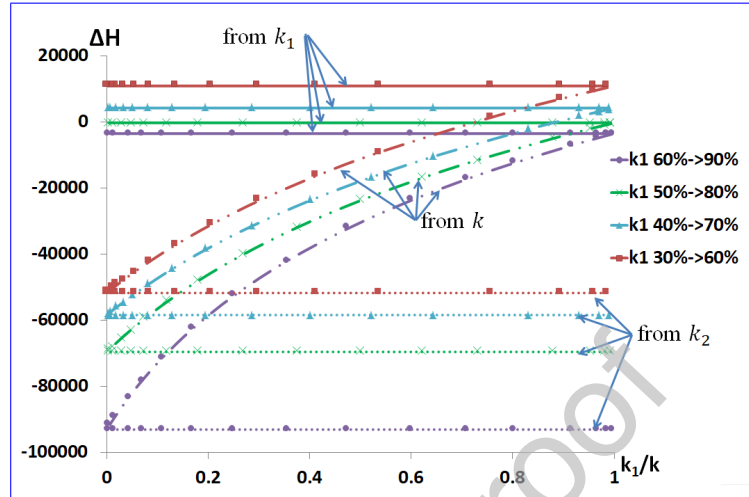


Figure 6: The calculated enthalpy changes when two adsorption sites are assumed and the retention factor is partitioned. Colors indicate different partitioning procedures [shown in the legend](#). The retention factor from which the calculation was made (k_1 , k_2 and k) is indicated [with arrows](#).

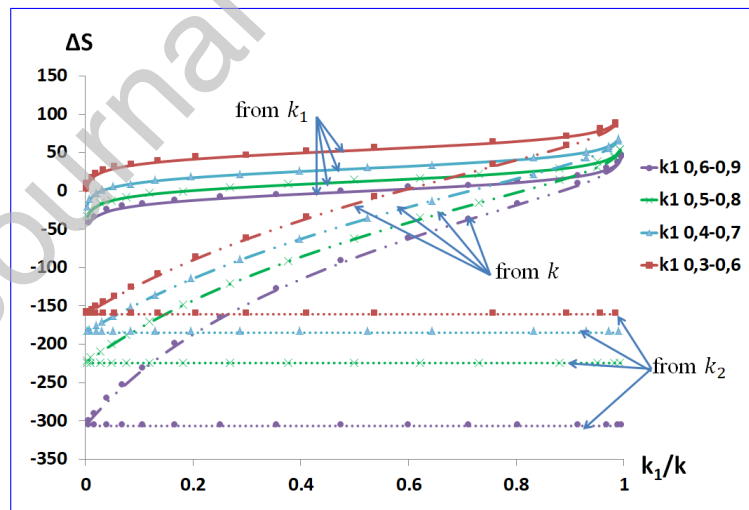


Figure 7: Calculated entropy changes when two adsorption sites are assumed and the retention factor is partitioned. Colors indicate different partitioning procedures [shown in the legend](#). The retention factor from which the calculation was made (k_1 , k_2 and k) is indicated [with arrows](#).

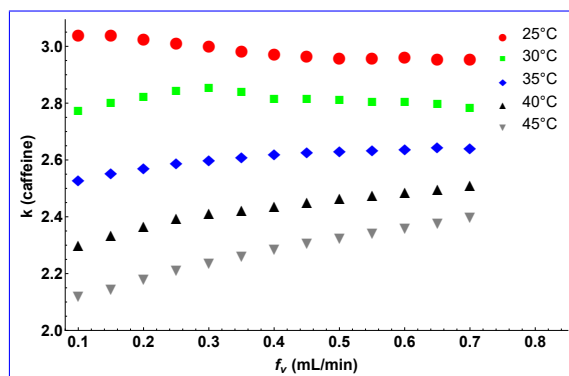


Figure 8: Dependence of the retention factor (k) on the flow-rate (F_V) on the Zorbax Eclipse Plus C18 column at 5 temperatures.

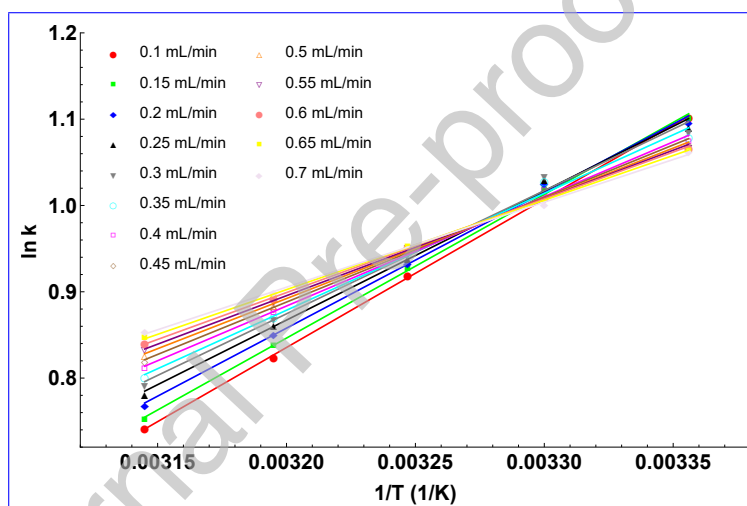


Figure 9: van't Hoff plots measured at various flow-rates on the Zorbax Eclipse Plus C18 column.

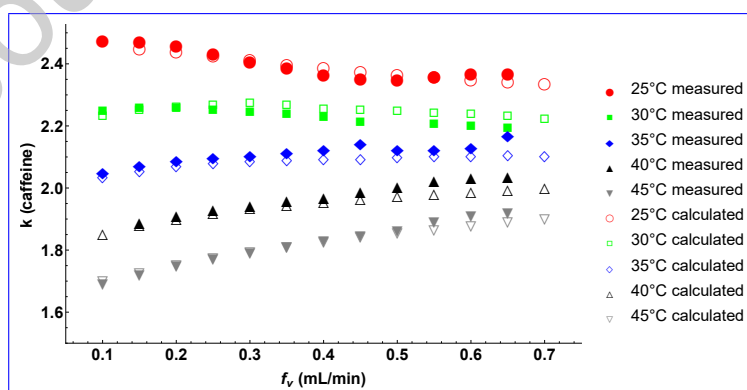


Figure 10: Dependence of the measured and calculated (Eq. 4) retention factors (k) at various flow-rates (F_V) on serially connected Zorbax C18 and Zorbax SB-CN columns at 5 temperatures.

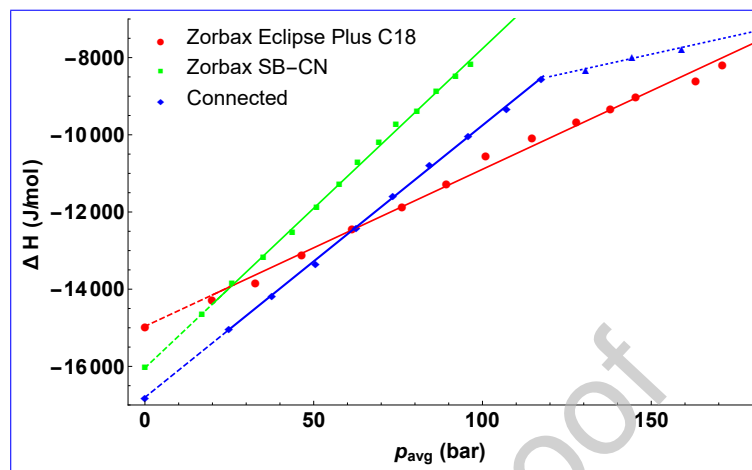


Figure 11: Dependence of the $\Delta H - \Delta H^\circ$ values calculated via the van 't Hoff plot on the average pressure drop along the columns for the two single columns (Zorbax Eclipse Plus C18 and Zorbax SB-CN) and when the same columns are serially connected.

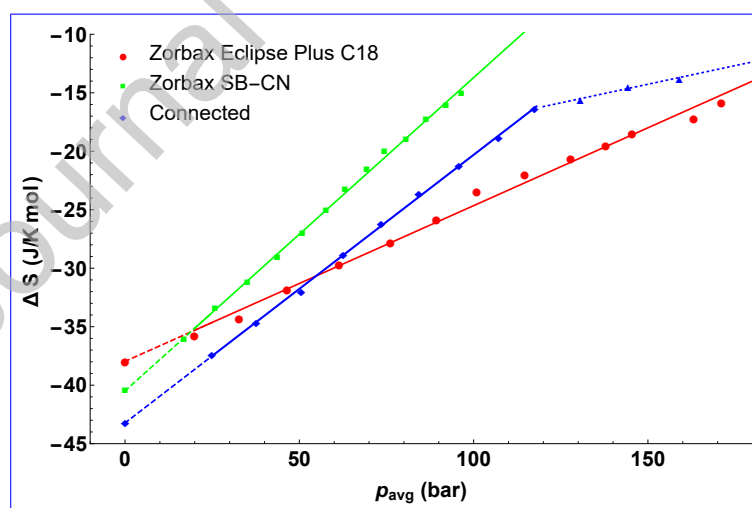


Figure 12: Dependence of the $\Delta S - \Delta S^\circ$ values calculated via the van 't Hoff plot on the average pressure drop along the columns for the two single columns (Zorbax Eclipse Plus C18 and Zorbax SB-CN) and when the same columns are serially connected.